Leukocyte analysis from WHIM syndrome patients reveals a pivotal role for GRK3 in CXCR4 signaling.

Karl Balabanian, Angélique Levoye, Lysiane Klemm, Bernard Lagane, Olivier Hermine, Julie Harriague, Françoise Baleux, Fernando Arenzana-Seisdedos, Françoise Bachelerie

Leukocyte analysis from WHIM syndrome patients reveals a pivotal role for GRK3 in CXCR4 signaling

Karl Balabanian,[1,2] Angélique Levoye,[1,2] Lysiane Klemm,[1,2] Bernard Lagane,[1,2] Olivier Hermine,[3] Julie Harriague,[1,2] Françoise Baleux,[4] Fernando Arenzana-Seisdedos,[1,2] and Françoise Bachelerie[1,2]

[1]INSERM U819, Paris, France. [2]Laboratoire de Pathogénie Virale Moléculaire, Institut Pasteur, Paris, France. [3]CNRS Unite Mixte de Recherche 8147, Hôpital Necker, Paris, France. [4]Unité de Chimie Organique, Institut Pasteur, Paris, France.

Leukocytes from individuals with warts, hypogammaglobulinemia, infections, and myelokathexis (WHIM) syndrome, a rare immunodeficiency, and bearing a wild-type *CXCR4* ORF (WHIM^{WT}) display impaired CXCR4 internalization and desensitization upon exposure to CXCL12. The resulting enhanced CXCR4-dependent responses, including chemotaxis, probably impair leukocyte trafficking and account for the immunohematologic clinical manifestations of WHIM syndrome. We provided here evidence that GPCR kinase-3 (GRK3) specifically regulates CXCL12-promoted internalization and desensitization of CXCR4. *GRK3*-silenced control cells displayed altered CXCR4 attenuation and enhanced chemotaxis, as did WHIM^{WT} cells. These findings identified GRK3 as a negative regulator of CXCL12-induced chemotaxis and as a candidate responsible for CXCR4 dysfunction in WHIM^{WT} leukocytes. Consistent with this, we showed that *GRK3* overexpression in both leukocytes and skin fibroblasts from 2 unrelated WHIM^{WT} patients restored CXCL12-induced internalization and desensitization of CXCR4 and normalized chemotaxis. Moreover, we found in cells derived from one patient a profound and selective decrease in GRK3 products that probably resulted from defective mRNA synthesis. Taken together, these results have revealed a pivotal role for GRK3 in regulating CXCR4 attenuation and have provided a mechanistic link between the GRK3 pathway and the CXCR4-related WHIM^{WT} disorder.

Introduction

WHIM syndrome is a rare combined immunodeficiency disorder characterized by disseminated human papillomavirus–induced warts, hypogammaglobulinemia, recurrent bacterial infections, and myelokathexis, a form of neutropenia associated with abnormal retention of mature neutrophils in the BM (1, 2). Many cases of WHIM syndrome have been linked to inherited heterozygous autosomal dominant mutations in the gene encoding CXCR4, a GPCR with a unique natural ligand, the chemokine stromal cell–derived factor 1/CXCL12 (SDF-1/CXCL12) (3). Binding of agonist to GPCR allows this family of receptors to associate with and signal through heterotrimeric G proteins by way of the exchange of GDP with GTP on the G protein α subunit, followed by the dissociation of the Gα from the Gβγ subunits, both of which exert regulation over various effectors (4).

WHIM-associated mutations of *CXCR4* lead to the expression of a receptor that displays an enhanced and prolonged activation of G proteins (reviewed in ref. 5). We previously reported that, in leukocytes from WHIM patients carrying a mutated CXCR4 receptor (CXCR4^{1013}), the increased G protein–dependent signaling is associated with the inability of CXCR4 to be uncoupled from G proteins (i.e., desensitized) and internalized in response to CXCL12 (6). In this genetic form of WHIM syndrome, impaired CXCR4 desensitization and internalization result from distal truncations of the receptor's carboxyterminal tail (C-tail) that remove potential phosphorylation sites involved in this attenuation process. A similar pattern of CXCR4 dysfunctions was observed in leukocytes from 2 unrelated subjects with full clinical form of WHIM syndrome and carrying a WT (WHIM^{WT}) *CXCR4* ORF (6). This indicates that the altered CXCR4-mediated signaling constitutes a common biologic trait of WHIM syndromes with different genetic causes. We thus hypothesized that WHIM^{WT} patients display anomalies affecting a gene product involved in the regulation of the agonist-dependent phosphorylation and/or the coupling of CXCR4 to the endocytic pathway. Ultimately, the resulting enhanced CXCR4-dependent signaling likely impairs leukocyte trafficking and accounts for the peculiar association of lymphopenia and myelokathexis with WHIM syndrome.

Members of the GPCR kinase (GRK) and arrestin families are pivotal participants in the canonical pathways leading to agonist-induced GPCR desensitization, a physiological feedback mechanism that rapidly uncouples the receptor from G proteins (7). GRKs phosphorylate Ser/Thr residues of intracellular loops and/or the C-tail of the agonist-activated receptor, a process that enhances the affinity of the receptor for the arrestins. The nonvisual β-arrestin1 and -2 are reported to interact with intracellular domains of CXCR4 and to regulate receptor desensitization and internalization (8–11). Seven GRKs are known, and among them, the 4 widely expressed members (GRK2, -3, -5, and -6) are supposed to regulate most GPCRs with overlapping receptor specificities (12, 13). Study of human diseases and genetically modified animals has recently revealed the physiological role of GRKs and pointed to some specificity of these kinases in regulating GPCR signaling (reviewed in ref. 14). However, to date, the GRKs responsible for agonist-promoted phosphorylation, desensitization, and/

Nonstandard abbreviations used: ActD, actinomycin D; C-tail, carboxyterminal tail; GRK, GPCR kinase; IB, immunoblot; LB, lysis buffer; P3, patient 3; SCR, scrambled control; WHIM, warts, hypogammaglobulinemia, infections, and myelokathexis.

Conflict of interest: The authors have declared that no conflict of interest exists.

Citation for this article: *J. Clin. Invest.* **118**:1074–1084 (2008). doi:10.1172/JCI33187.

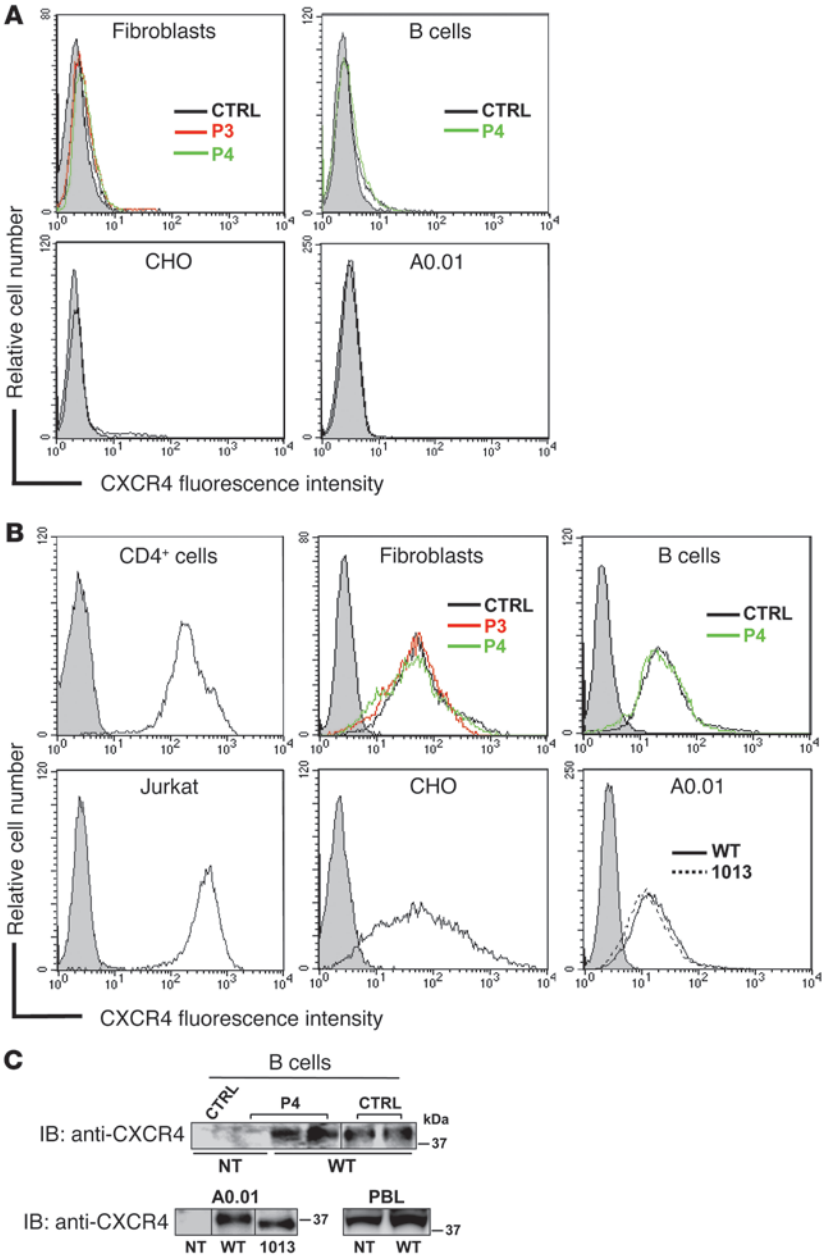

Figure 1
Analysis of CXCR4 expression in WHIM^{WT}-derived cells. (**A**) Membrane expression levels of endogenous CXCR4 in fibroblasts and EBV-B cells from healthy (CTRL), P3, and P4 subjects (upper panels) were determined by flow cytometry using the PE-conjugated 12G5 anti-CXCR4 mAb (white histograms) and compared with control staining measured in the CXCR4-negative CHO and A0.01 cell lines (lower panels). Gray histograms correspond to isotype control Ab. (**B**) Cell surface expression levels of endogenous CXCR4 in CD4$^+$ T cells from a healthy donor and the Jurkat T cell line (left panels) were compared with those of ectopically expressed CXCR4 following transduction of fibroblasts, EBV-B cells, CHO, and A0.01 cell lines (middle and right panels) with a WT or mutant (1013) *CXCR4* cDNA. (**C**) Lysates of EBV-B cells from CTRL and P4 subjects, A0.01 T cells, and PBLs from a healthy individual, either nontransduced (NT) or transduced with *CXCR4^{WT}* (WT) or *CXCR4^{1013}* (1013) cDNA, were incubated with the 12G5 anti-CXCR4 mAb precoated on γ-bind sepharose beads. Immunodetection of precipitated receptors using the SZ1567 anti-CXCR4 Ab revealed bands with molecular weights close to those expected for CXCR4^{WT} and CXCR4^{1013} (~39 and ~36 kDa, respectively). The thin vertical lines on the gel indicate that the lanes were run on the same gel but were noncontiguous. A representative experiment out of 2 (**C**) or >5 (**A** and **B**) independent determinations is shown.

or endocytosis of CXCR4 remain to be characterized, although some alterations of CXCR4 functions have been revealed in mice lacking *Grk6* (10, 15). In this work, we identify GRK3 as a key regulator of CXCR4 attenuation, the impaired activity of which in WHIM^{WT} cells accounts for the enhancement of CXCR4-mediated G protein–dependent responses.

Results

Selective CXCR4 dysfunctions in WHIM^{WT} cells. We derived forearm skin fibroblasts from WHIM^{WT} patient 3 (P3) and P4 and produced EBV-transformed B cell line from P4 (6), in order to set up cellular models to search for anomalies responsible for CXCR4 dysfunctions. Membrane expression levels of endogenous CXCR4 were barely detectable in all cell types (Figure 1A), as were other chemokine receptors, including CCR5, CCR7, CXCR2, CXCR5, and CXCR7, a newly identified receptor for CXCL12 (16) (data not shown). Following transduction, we analyzed the expression levels reached by CXCR4 at the membrane of either WHIM^{WT} and control fibroblasts and B cells or the CXCR4-negative CHO cell and A0.01 T cell lines. Flow cytometry analysis indicated that expression levels of CXCR4 were comparable at the surface of all transduced cell types and in the same range as the endogenous ones detected in primary CD4$^+$ T cells or Jurkat T cells (Figure 1B). In line with this, immunodetection of precipitated CXCR4 receptors was achieved only in transduced control and WHIM^{WT} EBV-B cells and increased in transduced PBL from a healthy subject. Immunoblot (IB) analysis revealed bands with a molecular weight close to that expected for CXCR4, as confirmed in A0.01 T cells expressing CXCR4 or its truncated C-tail counterpart CXCR4^{1013} (~39 and ~36 kDa, respectively) (Figure 1C).

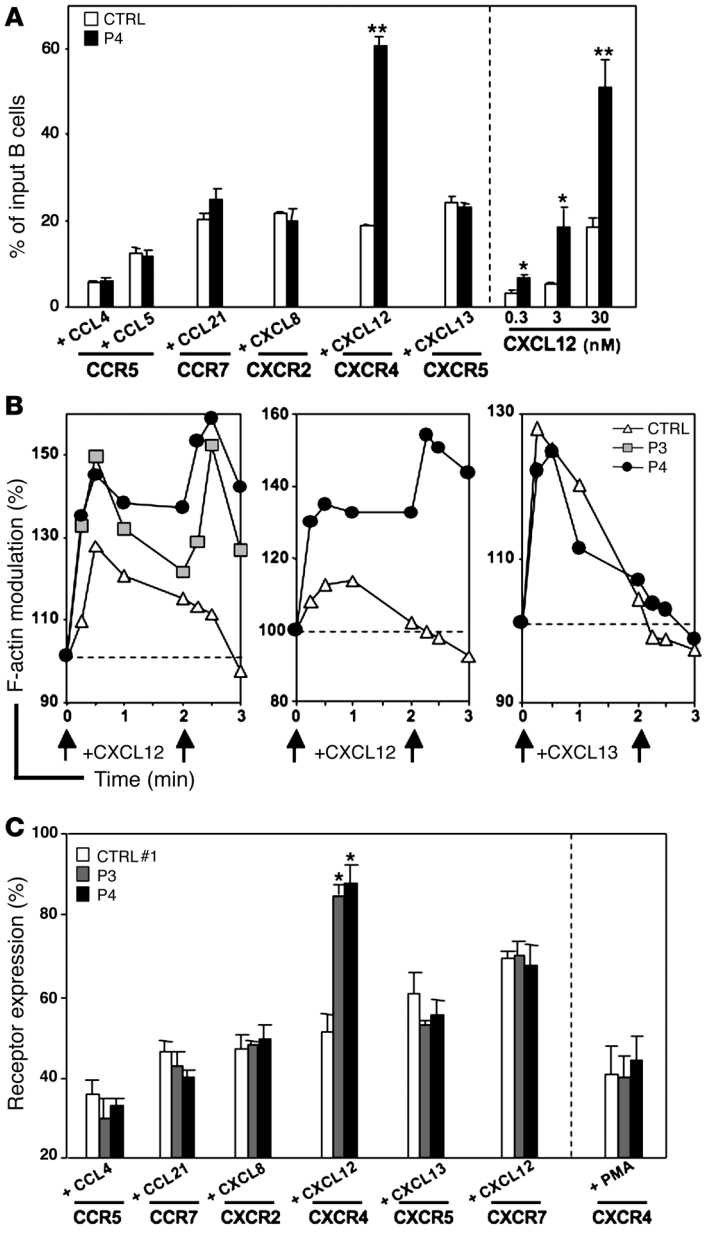

Figure 2
Selective alteration of CXCR4 functioning in WHIM^{WT} cells. (**A**) EBV-B cells from CTRL and P4 individuals were nucleoporated with 5 μg of plasmids encoding *CCR5*, *CCR7*, *CXCR2*, *CXCR4*, or *CXCR5* cDNA and assayed 15 h after transfection for chemotaxis using a Transwell system in response to the cognate chemokine (left section). Concentration-dependent migration of B cells expressing CXCR4 is shown in response to CXCL12 (right section). Results are expressed as a percentage of input B cells that migrated to the lower chamber. (**B**) Fibroblasts expressing CXCR4 (left panel) and B cells expressing either CXCR4 (middle panel) or CXCR5 (right panel) were tested for CXCL12- or CXCL13-triggered actin polymerization using FITC-phalloidin as a probe for intracellular F-actin. Arrows indicate chemokine stimulation. The baseline level of unstimulated cells was set as 100% (dotted line). (**C**) Cell surface expression of distinct chemokine receptors in control (CTRL#1) and WHIM^{WT} fibroblasts treated with 200 nM of the cognate agonist for 45 min at 37°C. Results indicate the amount of receptors that remains at the cell surface after incubation with agonist. Receptor expression at the surface of cells incubated in medium alone was set as 100%. Following transfection, expression levels of the different chemokine receptors were comparable at the surface of all unstimulated cell types as determined by flow cytometry (data not shown). Results represent the means ± SD of 3–5 independent experiments (**A** and **C**) or are representative of 3 independent determinations (**B**). $^{*}P < 0.05$; $^{**}P < 0.005$ compared with healthy subjects.

Various chemokine receptors were ectopically expressed in control and WHIM^{WT} fibroblasts and B cells to compare their functionality in response to their cognate ligand. Only WHIM^{WT} B cells expressing CXCR4 displayed stronger migratory responses, and at all of the ligand concentrations, thus indicating a higher efficiency of CXCL12 toward these cells (Figure 2A). Using CXCL12-triggered actin polymerization as an indicator of CXCR4-dependent G protein activation, we found that the enhanced chemotaxis of WHIM^{WT} cells was associated with a refractoriness of CXCR4 to be desensitized in response to CXCL12 (Figure 2B). In WHIM^{WT} cells, CXCR4 was also resistant to CXCL12-induced internalization but remained sensitive to treatment with the PKC inducer phorbol ester PMA (Figure 2C).

These findings show that WHIM^{WT} fibroblasts and EBV-B cells display the CXCR4 dysfunctions reported in the related patient primary leukocytes (6) and that other chemokine receptors, including CXCR7, are fully sensitive to their cognate ligand. Genetic analyses indicate the absence of mutation in the ORFs of *CXCR4*, *CXCR7*, and *CXCL12* in lymphoid (leukocytes and EBV-B cells) and/or nonlymphoid (skin fibroblasts) cells derived from P3 and P4, thus ruling out the possibility that abnormal CXCL12-dependent responses result from anomalies targeting one of these genes. We thus hypothesized that impaired CXCR4 desensitization and internalization in WHIM^{WT} cells rely on an abnormal gene product that directly or indirectly affects the agonist-dependent phosphorylation and/or the coupling of CXCR4 to the endocytic pathway.

β-arrestin–mediated CXCR4 internalization is preserved in WHIM^{WT} cells. The cellular levels of β-arrestin2 determine the extent of CXCR4 desensitization and internalization (8–10). Accordingly, we found that β-*arrestin2* expression in control fibroblasts significantly enhanced CXCL12-promoted internalization of CXCR4 (Figure 3A). Exogenous β-arrestin2 also preserved the ability to modulate CXCR4 endocytosis in fibroblasts and EBV-B cells (Figure 3A and data not shown, respectively) from WHIM^{WT} patients, in contrast to overexpressed β-arrestin1 (Figure 3B). Thus, these data support a modest role for β-arrestin1 in the regulation of CXCL12-promoted internalization of CXCR4 compared with that of β-arrestin2 (8, 9, 17). The question of whether impaired CXCR4 internalization in WHIM^{WT} cells relies upon a change in β-arrestin levels was addressed by IB analysis using Abs recognizing β-arrestin2 and/or β-arrestin1 (Supplemental Figure 1, A and B; supplemental material available online with this article; doi:10.1172/JCI33187DS1). We showed that steady-state levels of β-arrestin1 and β-arrestin2 proteins in WHIM^{WT} fibroblasts were similar to those detected in control cells (Figure 3, A and B). These findings were confirmed in EBV-B cells and primary leukocytes from both patients (Supplemental Figure 1C) and extended to the mRNA level (data not shown). As the ORFs of β-*arrestin1* and β-*arrestin2* were found to be wild type in all

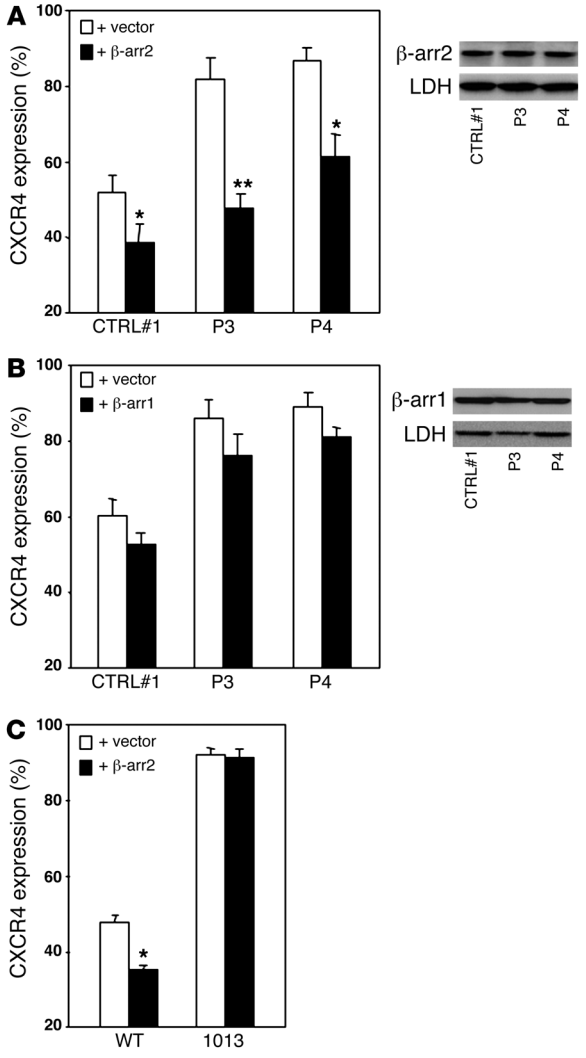

Figure 3

β-arrestin–mediated internalization of CXCR4. (**A** and **B**) CXCR4-transduced fibroblasts from healthy, P3, and P4 subjects were nucleoporated with 5 μg pN1-EGFP (vector), pβ-arrestin1–EGFP (β-arr1), or pβ-arrestin2–EGFP (β-arr2) and treated 15 h after transfection with 200 nM CXCL12 (left panels). Transfection rates >60% were obtained in all cell types as evaluated by flow cytometry. Results are expressed as percentage of CXCR4 expression (100% corresponding to CXCR4 expression at the surface of GFP^+-gated cells incubated in medium alone). Probing of protein extracts with an anti–β-arrestin1 or –β-arrestin2 Ab revealed proteins of expected molecular mass (~47 and ~46 kDa for β-arrestin1 and -2, respectively) in each sample (right panels). LDH (~35 kDa) was used as a loading control. (**C**) Membrane expression levels of $CXCR4^{WT}$ or $CXCR4^{1013}$ upon CXCL12 stimulation in CTRL#1 fibroblasts nucleoporated with 5 μg pN1-EGFP (vector) or pβ-arrestin2–EGFP. After transduction, $CXCR4^{WT}$ and $CXCR4^{1013}$ receptors were expressed at similar levels at the surface of unstimulated cells (data not shown). Results are means ± SD of >3 independent experiments (**A**–**C**) or are representative out of >3 independent determinations (**A** and **B**, right panels). $^*P < 0.05$; $^{**}P < 0.005$ compared with fibroblasts transfected with vector.

$WHIM^{WT}$ cell types, our results indicate a normal synthesis, stability, and translation of β-*arrestin* mRNAs in these cells. Altogether, these findings challenge the possibility that anomalies in β-*arrestin* account for the defective CXCR4 internalization in $WHIM^{WT}$ cells.

Moreover, the normal functioning of other chemokine receptors also indicates that the endocytic pathway downstream of β-arrestin recruitment is preserved in $WHIM^{WT}$ cells. GRK-mediated phosphorylation of C-tail Ser/Thr residues of CXCR4 (18), and thus C-tail integrity, are required for β-arrestin binding and receptor internalization (8, 19–21). Therefore, the impaired internalization of WHIM-associated C-tail–truncated CXCR4 mutants (6, 22) is likely due to the removal of critical C-tail phospho-acceptor sites (5, 8, 23, 24). Supporting this assumption, β-*arrestin2* overexpression, which largely exceeds the endogenous levels (Supplemental Figure 1B) and is known to overcome the need for GRK-dependent GPCR phosphorylation (25), did not promote the internalization of the WHIM-associated $CXCR4^{1013}$ receptor (Figure 3C), although it partly restored that of wild-type CXCR4 in patient-derived cells (Figure 3A). Collectively, these results led us to postulate that in $WHIM^{WT}$ cells a change in a gene product, such as GRK, that controls the agonist-promoted recruitment of β-arrestin2 to CXCR4 might account for the impaired receptor endocytosis.

CXCR4 internalization and desensitization are selectively regulated by GRK3. Recent works have revealed some specialization of the different GRKs in the regulation of GPCR signaling (26, 27), opening the possibility that this might be the case regarding the attenuation of CXCR4. In $WHIM^{WT}$ fibroblasts, similarly to control cells, expression of *GRK2*, *-5,* or *-6* had no or only a moderate effect on CXCL12-induced internalization of CXCR4 (Figure 4A). Interestingly, *GRK3* expression was highly effective in restoring normal CXCR4 endocytosis in fibroblasts from both patients (Figure 4, A and B). In contrast, *GRK3* expression did not normalize the internalization of the C-tail–truncated $CXCR4^{1013}$ receptor ectopically expressed in control or P3 fibroblasts (Figure 4B). An explanation for this observation is the removal of putative target sites for GRK3-mediated phosphorylation (Ser338/Ser339 and Ser341/Thr342 couples and Ser344) in the $CXCR4^{1013}$ receptor. These results strongly suggest that CXCR4 and GRK3 specifically interact so that receptor internalization can take place, thus opening the possibility that the capacity of exogenous GRK3 to restore internalization of CXCR4 in patient fibroblasts is related to interactions of the kinase with the receptor.

By knocking down *GRK3* mRNAs in control fibroblasts, we further investigated the apparent dependency of CXCR4 internalization upon GRK3 activity. In parallel, we also silenced *GRK2* mRNAs, as this kinase is closely related to GRK3 (28) and is found here to regulate significantly, albeit modestly, agonist-induced CXCR4 internalization in control cells (Figure 4A). Quantitative PCR and IB analyses revealed that siRNA duplexes efficiently and specifically depleted expression of each targeted GRK by more than 75% as compared with the scrambled control (SCR) siRNA (Figure 4C). As shown in Figure 4D, silencing of *GRK3* mRNAs led to a marked inhibition of CXCR4 internalization upon CXCL12 exposure, whereas suppression of *GRK2* expression did not affect this process. Taken together, our results highlight a previously unappreciated specialization of GRK3 in the regulation of CXCR4 internalization. We next determined whether, by regulating CXCR4 internalization, GRK3 also contributes to receptor desensitization. In $WHIM^{WT}$ fibroblasts, only *GRK3* expression was able to restore a normal CXCR4-dependent G protein activation following CXCL12 stimulation (Figure 4E). Collectively, these

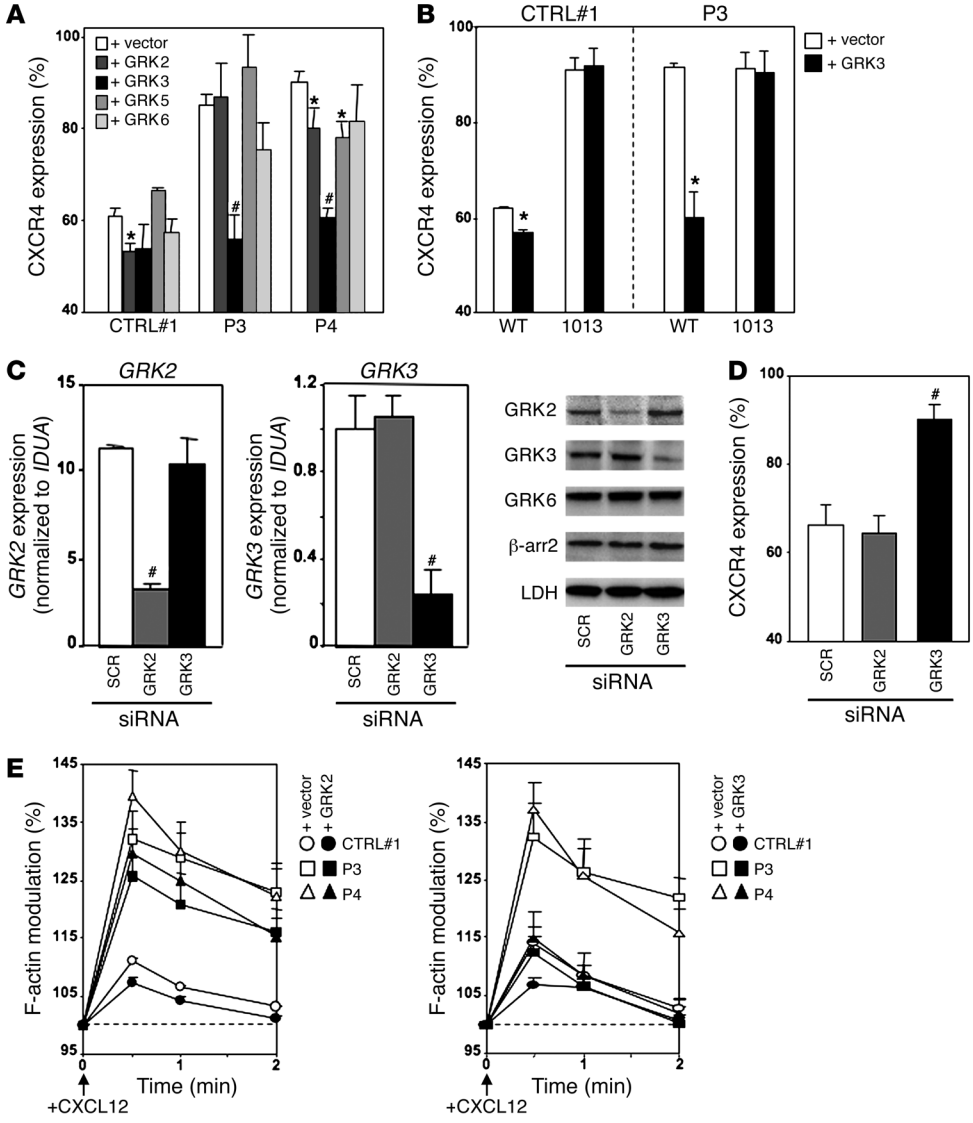

Figure 4

GRK3-mediated internalization and desensitization of CXCR4. (**A**) Aforementioned fibroblasts from CTRL#1, P3, and P4 subjects expressing CXCR4 were nucleoporated with 5 μg of either pcDNA1 (vector) or *GRK2*, *-3*, *-5*, or *-6* construct and treated 15 h after transfection with 200 nM CXCL12. We always controlled the efficiency of *GRK* overexpression by IB (Supplemental Figure 2C). (**B**) CXCL12-promoted internalization of $CXCR4^{WT}$ or $CXCR4^{1013}$ in fibroblasts from CTRL#1 and P3 nucleoporated with 5 μg of either pcDNA1 (vector) or plasmid encoding *GRK3* cDNA. (**C**) Expression of GRK products in fibroblasts from healthy subjects nucleoporated with 5 μg SCR, *GRK2*, or *GRK3* siRNAs. Three days after transfection, *GRK* mRNA levels were assessed by quantitative PCR (left and middle panels) and normalized to those of *IDUA*. IB of proteins from whole-cell lysates either with an anti-GRK2/3 mAb (data not shown) or an anti-GRK2 or anti-GRK3 Ab (right panel) revealed proteins of expected molecular mass (~80 kDa). *GRK2* or *-3* siRNAs had no effect on expression levels of endogenous GRK6 or β-arrestin2 (molecular mass ~65 and ~46 kDa, respectively), as detected using selective Abs (Supplemental Figures 1 and 2). (**D**) Cell surface expression levels of CXCR4 in *GRK2* or *-3* siRNA-transfected fibroblasts treated with CXCL12. *GRK2* or *-3* siRNAs had no effect on expression levels of CXCR4 at the membrane of unstimulated cells (data not shown). (**E**) CXCR4-transduced fibroblasts from CTRL#1, P3, and P4 individuals were nucleoporated with 5 μg of pcDNA1 (vector) or *GRK2* or *-3* construct and tested for CXCL12-triggered actin polymerization. Results are means ± SD of 3–6 independent experiments (**A** and **B**; **C**, left and middle panels; and **D** and **E**) or are representative of >5 independent determinations (**C**, right panel). $^{*}P < 0.05$; $^{\#}P < 0.005$ compared with fibroblasts transfected with vector (**A** and **B**) or SCR siRNAs (**C** and **D**).

results reveal a pivotal role for GRK3 in the regulation of CXCR4 desensitization and internalization and further point to GRK3 as a candidate responsible for the impaired CXCR4 attenuation in $WHIM^{WT}$ cells. Supporting this assumption, *GRK3*-silenced control cells displayed an impaired CXCR4 endocytosis upon CXCL12 exposure, as do $WHIM^{WT}$ cells. Conversely, *GRK3* expression in $WHIM^{WT}$ cells normalized CXCR4 desensitization and endocytosis. These observations argue in favor of a quantitative or qualitative change in GRK3 in $WHIM^{WT}$ cells.

Differential steady-state levels of GRK3 products in $WHIM^{WT}$ leukocytes. To investigate whether $WHIM^{WT}$ cells display a quantitative change in GRK3 proteins, we assessed by IB the levels of

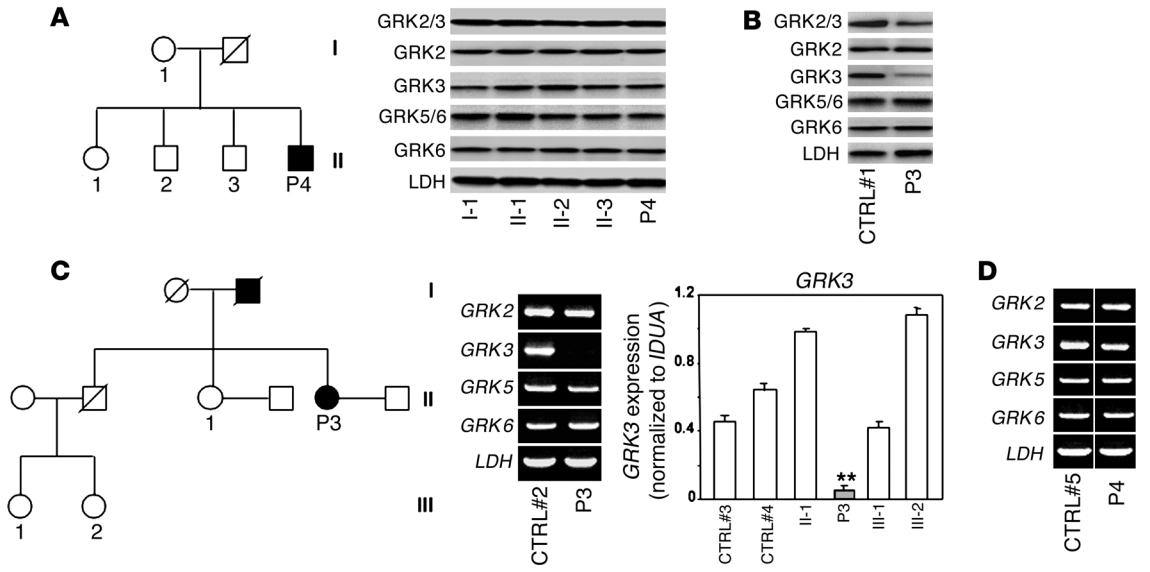

Figure 5

Reduced levels of GRK3 products in P3 leukocytes. (**A** and **B**) The steady-state levels of GRK proteins in leukocytes from P4 (**A**) and P3 (**B**) were compared with those obtained in leukocytes from family members and a healthy individual (CTRL#1), respectively. Total protein extracts (20 μg/lane) were analyzed by IB using an anti-GRK2/3, -GRK2, -GRK3, -GRK5/6, or -GRK6 Ab. (**C** and **D**) The steady-state levels of *GRK* transcripts in leukocytes from P3 (**C**) and P4 (**D**) were compared by PCR with those obtained in leukocytes from family members and healthy individuals (CTRL#2–5). Semi-quantitative (**C**, middle panel, and **D**) and real-time (**C**, right panel) PCRs were performed using specific primers flanking the full *GRK* ORFs or within them, respectively. One band corresponding to amplified *LDH* (~1.3 kb), *GRK2* (~2.2 kb), *GRK3* (~2.1 kb), *GRK5* (~1.8 kb), or *GRK6* (~1.8 kb) cDNA products was detected in each sample by semi-quantitative PCR. The thin horizontal lines in the gel indicate that the lanes were run on the same gel but were noncontiguous. Results are from 1 representative experiment of 3 (**A**–**D**) or are means ± SD of 3 independent determinations performed in triplicate (**C**, right panel). $^{**}P < 0.005$ compared with III-1 individual.

GRK2, -3, -5, and -6 in whole-cell lysates from primary leukocytes isolated from P3, P4, and healthy subjects including members of P4's family (Figure 5A). No change in GRK3 levels was detected in leukocytes from P4 (Figure 5A). In contrast, the levels of GRK3 in leukocytes from P3 were profoundly reduced compared with controls, whereas the steady-state levels of GRK2, -5, and -6 were normal as detected with Abs that react specifically with GRK2 or -6 or the GRK5/6 pair (Figure 5B and Supplemental Figure 2, A and C). The decrease in GRK3 protein levels, also confirmed in P3 fibroblasts (Figure 6A), was accessed using a mAb that reacts with GRK2 and -3 proteins (>60% reduction as compared with control cells) (Supplemental Figure 2, C and D), both readily distinguished as a doublet (Supplemental Figure 2B), or an Ab that selectively recognizes GRK3 proteins (~90% reduction as compared with controls) (Supplemental Figure 2, A and D).

To determine whether the decrease in GRK3 proteins identified in P3 leukocytes was mirrored at the mRNA level, total RNA was isolated from P3 and control leukocytes, and the steady-state levels of *GRK3* transcripts were assessed by PCR analysis. Using semiquantitative PCR, we found that the band corresponding to the amplified *GRK3* cDNA product was barely detectable in P3 leukocytes as compared with control cells, suggesting a drastic reduction of *GRK3* transcript amounts in P3 cells (Figure 5C). In contrast, the steady-state levels of *GRK2*, *-5,* and *-6* mRNAs were similar in P3 and control leukocytes. Amounts of *GRK* transcripts in P4 leukocytes were not different from those detected in control cells as shown by semiquantitative PCR analysis (Figure 5D). We then set up real-time PCR analysis to quantify levels of *GRK3* mRNAs in P3 leukocytes as compared with those detected in 5 independent healthy individuals, among which 3 are family members (Figure 5C). The steady-state levels of *GRK3* transcripts in control individuals displayed over a large range (Figure 5C). This observation is probably the consequence of an inter-individual variability that is also revealed by a similar comparative analysis performed in leukocytes from P4 and healthy members of P4's family (Supplemental Figure 3). However, *GRK3* mRNA levels were out of range in P3 leukocytes (Figure 5C) and only minute amounts were detectable in accordance with the semiquantitative PCR analysis. We also confirmed by real-time PCR that the steady-state levels of other *GRK* mRNAs were quantitatively unaffected in P3 cells (data not shown). Thus, these results indicate that the marked alteration in GRK3 protein levels in P3 leukocytes correlates with a selective decrease at the mRNA level. Additionally, our findings strongly suggest that the decreased steady-state level of GRK3 proteins in P3 leukocytes results from an alteration in a (post-)transcriptional mechanism rather than in protein stability.

Defective GRK3 mRNA expression in P3 fibroblasts. RNA stability studies were set up in patient-derived fibroblasts, which constitute a more homogenous cell system than leukocytes. As shown in Figure 6A, fibroblasts from P3 displayed a selective reduction (>75%) in GRK3 protein levels relative to controls, as did leukocytes (see Figure 5B). We also confirmed that the steady-state levels of GRK2, -3, -5, and -6 proteins were unaffected in fibroblasts and EBV-B cells (data not shown) from P4. Of note, exogenously expressed GRK3, which was found to restore CXCR4 internalization and desensitization in P3 and P4 fibroblasts (Figure 4, A, B, and E), reached similar levels among control and patient fibroblasts that largely exceeded the endogenous ones (Supplemental Figure 2C). Whereas the amounts

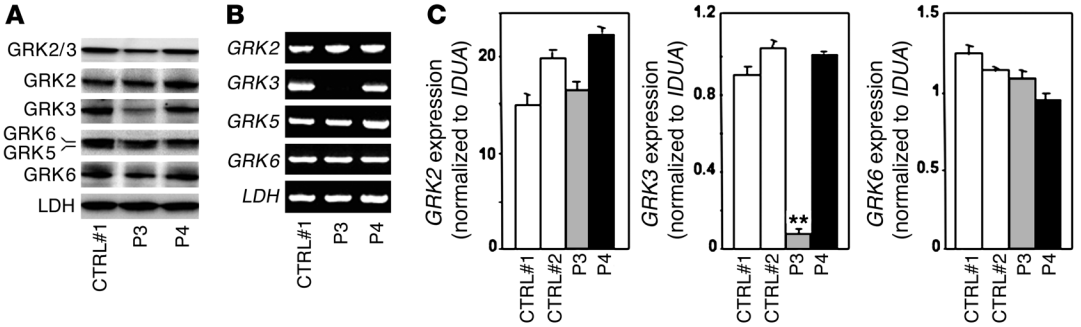

Figure 6
Differential steady-state levels of GRK3 products in WHIM^{WT} fibroblasts. Analyses of GRK protein and mRNA levels in fibroblasts from P3, P4, and 2 independent healthy subjects (CTRL#1 and #2) were performed by IB (**A**), semi-quantitative (**B**), and real-time (**C**) PCRs as described in the legend of Figure 5. Results are from 1 representative experiment of 6 (**A** and **B**) or are means ± SD of 3 independent determinations performed in triplicate (**C**). $^{**}P < 0.005$ compared with CTRL#1.

of *GRK* mRNAs were unaltered in P4 fibroblasts compared with control ones, we observed a drastic decrease (>85%) of *GRK3* transcripts in P3 fibroblasts (Figure 6, B and C). A single *GRK3* cDNA product was amplified by PCR using specific primers flanking the full ORF in patient-derived leukocytes (Figure 5) and fibroblasts (Figure 6). Double-strand sequencing of amplified products revealed no mutation either in the *GRK3* ORF or in those of *GRK2*, *-5*, and *-6*.

We speculated that the reduced level of *GRK3* transcripts in P3 cells might result from 2 mechanisms not mutually exclusive: inefficient mRNA synthesis or increased mRNA degradation. A time course of *GRK3* mRNA stability was performed in the presence of the transcriptional inhibitor actinomycin D (ActD) in fibroblasts from P3, P4, and 2 healthy subjects. The estimated half-life (>3 h) of a stable mRNA species, *lactate dehydrogenase* (*LDH*), was found to be similar in all cell types (Figure 7A). *GRK3* mRNAs were found to have a short half-life (~1 h), and their stabilities were in the same range in both control- and patient-derived fibroblasts (Figure 7B). These findings rule out the possibility that an impaired mRNA stability accounts for the decrease of *GRK3* transcripts in P3 fibroblasts, and argue in favor of an altered *GRK3* transcription. We thus set up pulse/chase ActD experiments and determined that a 4-hour treatment with ActD was sufficient to deplete *GRK3* mRNAs (<15% of the pretreatment levels) in all cell types (Figure 7C). After 4 h of ActD chase, the level of *GRK3* mRNAs was fully recovered in P4 and control fibroblasts, whereas it only reached 50% of the pretreatment levels in P3 fibroblasts. Taken together, these results strongly suggest that the decreased level of GRK3 proteins in P3 cells primarily results from an impaired *GRK3* mRNA synthesis and ultimately leads to defective CXCR4 attenuation.

GRK3 negatively regulates CXCL12-promoted cell migration. We hypothesized that the enhanced CXCL12-promoted chemotaxis of P3 cells, previously proposed to rely on the refractoriness of CXCR4 to be both desensitized and internalized (6), could be normalized upon *GRK3* expression. To address this issue, leukocytes from healthy and P3 subjects were transfected either with a control vector or a plasmid encoding *GRK3* cDNA (Supplemental Figure 2D). Confirming our previous findings, CD4$^+$ T cells from P3 displayed a stronger chemotactic response toward a CXCL12 gradient relative to controls

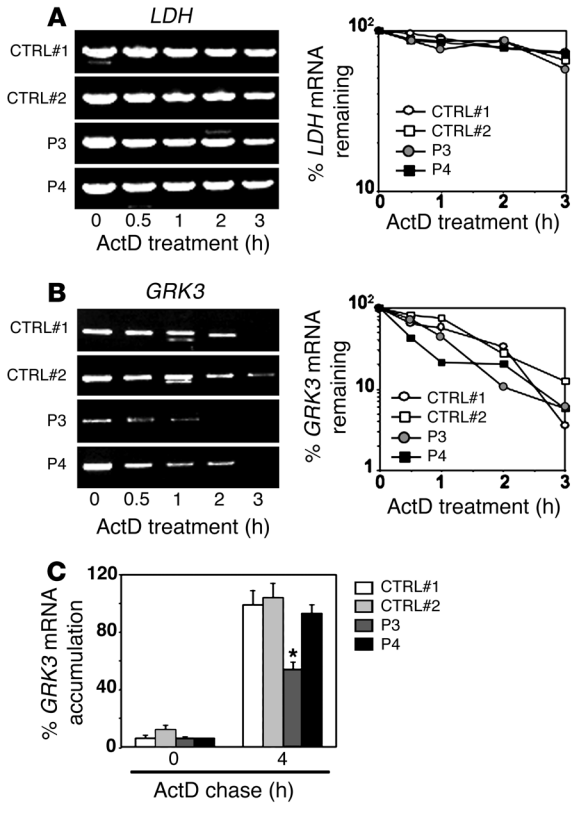

Figure 7
Expression and stability of *GRK3* mRNAs in WHIM^{WT} fibroblasts. Fibroblasts from P3, P4, and healthy subjects were incubated with 10 μg/ml ActD (treatment) for the indicated times (**A** and **B**) or for 4 h and further cultured for 4 h in the absence of ActD (chase) (**C**). At the indicated times, total RNA was extracted and semi-quantitative PCRs were performed using specific primers flanking the full *LDH* or *GRK3* ORF. Amplified cDNA products were run on 1% agarose gels, detected by ethidium bromide staining, and quantified by computed-assisted densitometry using the ImageJ 1.34 software (NIH). Results are from 1 representative experiment out of 3 (**A** and **B**) or are means ± SD of 3 independent determinations (**C**) and indicate the amount of mRNAs that remained after incubation with ActD (**A** and **B**) or that accumulated in the course of ActD chase (**C**). Transcript levels in fibroblasts incubated in medium alone were set as 100%. Kinetics of *LDH* mRNA appearance were comparable in all cell types (data not shown). $^{*}P < 0.05$.

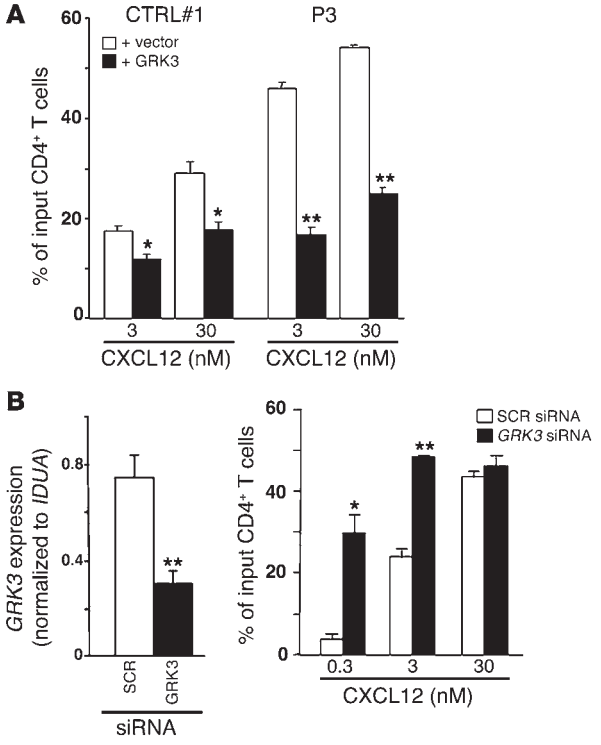

Figure 8
Consequences of *GRK3* expression or knock-down on CXCL12-promoted chemotaxis. (**A**) Leukocytes from healthy (CTRL#1) and P3 subjects were nucleoporated with 5 μg of either pcDNA1 (vector) or plasmid encoding *GRK3* cDNA and assayed 15 h after transfection for chemotaxis in response to CXCL12. (**B**) IL-2–expanded leukocytes that contained >95% $CD25^+$ blasted T cells, as evaluated by flow cytometry, from independent healthy individuals were nucleoporated with 5 μg SCR or *GRK3* siRNAs. Two days after transfection, leukocytes were tested for their ability to migrate in response to CXCL12 (right panel). Transmigrated cells recovered in the lower chamber were stained with mAbs specific for CD3 and CD4 antigens and counted by flow cytometry. Results, expressed as a percentage of input $CD4^+$-gated T cells that migrated to the lower chamber, are representative of those obtained in $CD8^+$-gated T cells. *GRK3* transcript levels were evaluated by quantitative PCR and normalized to those of *IDUA* (**B**, left panel). Inhibition or increase of *GRK3* expression had no effect on cell surface expression of CXCR4. Results are from 1 representative determination of 2 performed in triplicate (**A**) or are means ± SD of 3 independent determinations performed in duplicate (**B**, right panel) or in triplicate (**B**, left panel). $^*P < 0.05$; $^{**}P < 0.005$ compared with leukocytes transfected with vector or SCR siRNAs.

(Figure 8A). We found that *GRK3* expression significantly reduced CXCL12-promoted migration of control T cells (30%–40% inhibition as compared to cells transfected with vector), suggesting that GRK3 plays a negative role in the regulation of this process. Consistent with this, *GRK3* expression in leukocytes from P3 permitted the restoration of normal CXCL12-induced chemotactic responses.

By knocking down *GRK3* mRNAs in leukocytes from healthy subjects, we further investigated the dependency of CXCR4-mediated cell migration upon GRK3 activity. As determined by real-time PCR, *GRK3* siRNA duplexes efficiently reduced the levels of *GRK3* transcripts by more than 60% (Figure 8B). Addition of CXCL12 resulted in a dose-dependent chemotaxis of SCR siRNA-transfected $CD4^+$ T cells (Figure 8B). Supporting a negative role for GRK3 in CXCL12-promoted chemotaxis, we found that the sensitivity of *GRK3*-silenced $CD4^+$ T cells to CXCL12 was strongly increased. This process was associated with a decrease in the maximal effective concentration of CXCL12.

Discussion

Investigation of the molecular basis of CXCR4 dysfunctions in 2 patients suffering from the genetic form of WHIM syndrome not associated with *CXCR4* mutation reveals a surprising dependency of CXCR4 functioning upon GRK3 activity. For instance, our data demonstrate a pivotal role for GRK3 in CXCL12-promoted desensitization and internalization of CXCR4. They also point to alterations in GRK3 activity in patient-derived cells that likely account for the CXCR4 dysfunctions. Several observations support this possibility. First, control cells knocked down for *GRK3* mRNAs displayed impaired CXCR4 attenuation and enhanced chemotaxis in response to CXCL12, as do $WHIM^{WT}$ cells. Second, *GRK3* expression in $WHIM^{WT}$ cells restored the capacity of CXCR4 to be desensitized and internalized in response to CXCL12. Finally, and perhaps most importantly, we revealed in cells derived from one patient a selective decrease in GRK3 products that likely arises from impaired mRNA synthesis and the correction of which led to a normalized chemotaxis.

CXCL12-promoted desensitization and internalization of CXCR4 is thought to be dependent upon binding of β-arrestin to the GRK-phosphorylated receptor (8, 9, 18). Our data challenge the possibility that β-arrestin1 or β-arrestin2 per se could be impaired in patient-derived cells and rather point to GRK3 activity as the limiting step. In $WHIM^{WT}$ and control cells, the steady-state levels of β-arrestin products were found to be similar (Figure 3, A and B, and Supplemental Figure 1C), as well as the internalization of chemokine receptors other than CXCR4 (Figure 2C). These results suggest that the endocytic pathway downstream of β-arrestin recruitment to the receptors is preserved in $WHIM^{WT}$ cells. In line with this, ectopically expressed β-arrestins, and most particularly β-arrestin2, had the ability to modulate CXCR4 internalization (Figure 3). However, this effect was partial, whereas for exogenous GRK3, it was total (Figure 4, A and B). Indeed, *GRK3* expression overcame the resistance of CXCR4 to internalize in response to CXCL12 in patient-derived cells, including those from P4, which displayed normal steady-state levels of GRK3 products (Figures 5 and 6). Chemokine receptor internalization is facilitated by *GRK* expression, as previously reported for CXCR4 upon transfection of *GRK2* cDNA in HEK 293T cells (8, 9) and here in primary fibroblasts (Figure 4A). The fact that *GRK2* silencing did not modulate CXCL12-induced internalization of CXCR4 in control fibroblasts (Figure 4D) suggests a minor contribution of this kinase to this process and makes it likely that GRK3 activity is sufficient for receptor phosphorylation in those cells. Consistent with this, *GRK3* silencing impaired CXCR4 internalization in control cells, indicating that neither endogenous GRK2 nor GRK5 or -6 substituted for the loss of GRK3.

Endogenous GRK3 has been shown to mediate the agonist-dependent phosphorylation and internalization of other GPCRs, such as

angiotensin II and V2 vasopressin receptors (26, 27). Analyses of *GRK3*-deficient mice reveal a physiological role for Grk3 in the regulation of olfactory, M_2/M_3 muscarinic and kappa opioid receptor activities (29–31). However, whether *Grk3* deficiency affects GPCRs also involved in the immune system homeostasis has not been investigated. Here, by the use of alternative approaches (overexpression combined with siRNA methods), we uncover a selective role for GRK3 in the regulation of CXCL12-promoted attenuation of CXCR4 that likely implicates agonist-induced C-tail phosphorylation and the subsequent recruitment of β-arrestin2 to phosphorylated receptors. In line with this, the failure of either β-*arrestin2* or *GRK3* overexpression to correct impaired CXCL12-induced internalization of the WHIM-associated $CXCR4^{1013}$ receptor was consistent with the removal of phosphorylation sites in the C-tail truncated receptor that prevents the physical interaction of the kinase with the receptor (Figure 3C and Figure 4B). GRK3 and the structurally related GRK2 have the reported ability to interact with the activated GTP-bound form of some Gα proteins, notably Gαq and Gα11, and to accelerate their intrinsic GTPase activity (reviewed in ref. 28). CXCR4 is thought to generally activate Gαi proteins, but it also displays the capacity to couple to Gα12/13 (32, 33) or Gαq proteins (34, 35). This opens the possibility that the binding of GRK3 to G proteins might contribute in some conditions to CXCR4 desensitization in a phosphorylation and/or β-arrestin–independent manner.

The enhanced CXCL12-promoted chemotaxis displayed by P3 T cells (Figure 8A) likely arises from the drastic diminution of GRK3 products that characterizes P3-derived cells (Figures 5 and 6). This assumption is supported by the fact that *GRK3* expression in P3 T cells was sufficient to correct altered CXCL12-induced chemotaxis, and conversely that *GRK3* silencing in control T cells results in a WHIM-like phenotype (Figure 8). The mechanism by which GRK3 levels fine-tune CXCL12-promoted cell migration might involve the pivotal role of GRK3 in promoting β-arrestin2–mediated CXCR4 desensitization. In addition to desensitization, recent studies suggest that β-arrestin2 contributes to chemotaxis by virtue of its ability to serve as scaffold for signaling molecules, including members of the MAPK family (4). β-arrestin2 was shown to positively modulate CXCR4-mediated chemotaxis of mouse and human cells (10, 36). Thus, changes in GRK3 activity in $WHIM^{WT}$ cells may indirectly modulate the ability of β-arrestin2 to scaffold CXCR4-mediated signaling pathways. Recent findings indicate that different GRKs may set in motion distinct functions of GPCR-bound β-arrestin (26, 27, 37, 38), opening the possibility that a specialization of GRKs also takes place in the regulation of β-arrestin2–dependent CXCR4 signaling. For instance, studies from *Grk6*-deficient mice suggest a positive contribution of this kinase to the CXCL12-induced chemotaxis of T cells, whereas Grk6 appears to play an opposite role in neutrophils (10, 15). These results, if extended to the regulation of CXCR4-mediated signaling in human cells, would open the possibility that GRK6 and GRK3 differentially regulate CXCR4 activities. In $WHIM^{WT}$ cells, our results indicate that GRK6 is not dysregulated and highlight a role for GRK3 dysfunctions per se in the enhanced CXCL12-promoted chemotaxis.

We reveal that functional CXCR4-related defaults in P3 cells result from a dramatic decrease in GRK3 proteins, likely due to an impairment in mRNA expression but not stability (Figure 7). The relatively short half-life of *GRK3* mRNA species is consistent with the reported tight regulation of the *GRK3* promoter by various inducers, including κ-opioid agonists, corticotropin-releasing factor, epinephrine, or the cytokine GM-CSF (39–43). Collectively, these observations suggest that the defective *GRK3* mRNA expression in P3 cells arises from an impaired synthesis, either directly due to a polymorphism in transcriptional regulatory regions or indirectly due to the altered expression of a transcription factor that modulates *GRK3* expression. Several SNPs were identified in the putative promoter region of *GRK3*, which may affect the regulation of gene expression, and were associated with bipolar disorder in families of northern European Caucasian ancestry (44, 45). We did not identify any specific SNP in the minimal putative promoter region of *GRK3* in P3 cells. Therefore, cloning and functional characterization of the whole *GRK3* transcriptional regulatory sequence may help to define mechanisms by which *GRK3* expression is fine-tuned in P3 cells.

The molecular mechanism accounting for the impaired CXCR4 attenuation in P4 cells is predicted to arise upstream β-arrestin2 recruitment to CXCR4 and coupling of the receptor to the endocytic pathway. Several aspects of our findings make it more likely that the defect occurs through a direct dysregulation of GRK3 subcellular localization and/or activity rather than a GRK3-unrelated process of receptor downregulation. In particular, the resistance of the $CXCR4^{1013}$ receptor to internalize upon CXCL12 stimulation, even in the presence of large amounts of GRK3 (Figure 4B), strongly suggests that GRK3 physically interacts with the C-tail of CXCR4. So, the selective effect of overexpressed GRK3 in correcting impaired CXCR4 internalization in P4 cells (Figure 4A) is believed to result from the restoration of specific interactions of the kinase with the receptor and thus to overcome a deficiency in GRK3 activity. The normal production, stability, and translation of *GRK3* mRNAs in P4 cells (Figures 5–7), combined with the absence of mutation in the *GRK3* ORF, challenge the possibility of intrinsic changes in GRK3 proteins. Additionally, these observations suggest that GRK3-related CXCR4 dysfunctions arise from different genetic anomalies in P3 and P4 subjects with full clinical form of WHIM syndrome. Based on recent advances in our knowledge of the GRK interactome (reviewed in ref. 28), we speculate that alteration in one of GRK's binding partners may lead to impaired GRK3 localization and/or activity in P4 cells. A fuller understanding of the functioning of GRK3 should provide insight into the biology of the CXCL12/CXCR4 axis and likely into the aberrant leukocyte trafficking in the course of WHIM syndrome.

Methods

Antibodies, reagents, and cells. Immunostainings were performed using the FITC-conjugated anti-human CD3 mAb (clone SK7), the PE-conjugated anti-human mAbs specific for CCR5 (clone 2D7), CCR7 (clone 3D12), CXCR2 (clone 48311.211), CXCR4 (clone 12G5), and CXCR5 (clone 51505.111) as well as the APC-conjugated anti-human CD4 (clone RPA-T4) mAb. All mAbs were purchased from BD Biosciences. The binding of the mouse anti-human RDC1/CXCR7 mAb (clone 9C4, provided by M. Thelen, Institute for Research in Biomedicine, Bellinzona, Switzerland) was detected as described (16). Unless specified, MIP-1β/CCL4, SDF-1/CXCL12, and RANTES/CCL5 and IL-8/CXCL8 (both from R&D Systems) were used at 30 nM, whereas 6Ckine/CCL21 and BCA-1/CXCL13 (R&D Systems) were used at 60 nM and 100 nM, respectively. PMA (Sigma-Aldrich) was used at 200 nM.

PBLs were isolated from heparin-treated blood samples of healthy individuals and $WHIM^{WT}$ patients P3 and P4 as previously described (6) and cultured in RPMI 1640 medium supplemented with 10% FCS, 10 mM HEPES, penicillin (100 U/ml), and streptomycin (100 μg/ml) (complete RPMI medium). When required, PBLs from healthy subjects were either nega-

tively enriched for $CD4^+$ T cells as previously described (46) or incubated for 24 h with phytohemagglutinin (1 μg/ml; Sigma-Aldrich) followed by 6 days with IL-2 (20 ng/ml; PeproTech) for blasting. The A0.01 T cell (from H.T. He, Centre d'Immunologie de Luminy, Marseille, France) and Jurkat cell (ATCC) lines were maintained in complete RPMI medium. The CHO K1 cell line (ATCC) was cultured in complete HAM F-12 medium. Dermal fibroblasts, isolated and expanded from healthy and $WHIM^{WT}$ skin biopsies, were maintained in complete DMEM. EBV-transformed B cell lines derived from healthy individuals and P4 were cultured in complete RPMI medium supplemented with 50 μM 2-mercaptoethanol. The marked B cell lymphopenia affecting P3 did not permit us to generate a B cell line. This study was approved by the Direction Médicale et Santé Publique, Institut Pasteur, and all subjects gave informed consent for this investigation.

Transfection and functional assays. The human SMARTpool SCR (siCONTROL non-targeting#1), *GRK2*, and *GRK3* siRNA duplexes (Dharmacon); the pN1-EGFP, pβ-arrestin1–EGFP, and pβ-arrestin2–EGFP plasmids (provided by S. Marullo, Institut Cochin, Paris, France); the pcDNA1 encoding bovine *GRK2*, *-3*, or *-5* or human *GRK6* cDNA (gift from M. Oppermann, University of Göttingen, Germany); the pcDNA3 encoding human *CXCR2* cDNA and the pSRαpuro-CCR7 and -CXCR2 plasmids (gift from B. Moser, Theodor-Kocher Institute, Bern, Switzerland); and the lentiviral-derived pTRIP vectors (gift from P. Charneau, Unité de Virologie Moléculaire et de Vectorologie, Institut Pasteur, Paris, France) encoding human *CCR5*, *CXCR4*, *$CXCR4^{1013}$*, or *CXCR7* cDNA were transfected as specified in the legends to Figures 1–4 and Figure 8. Transient expression was achieved using amaxa Nucleofector technology, and stable expression was obtained using a lentiviral-based strategy as previously described (6). Receptor internalization, actin polymerization, and chemotaxis assays were performed as previously described (6, 46). Statistical analyses consisted of unpaired 2-tailed Student *t* tests and were conducted with the Prism software (GraphPad).

RT-PCR analysis. Total cellular RNA was extracted using the RNeasy kit (QIAGEN Sciences) and reverse transcribed (Superscript II, BD Biosciences Clontech) by extension of oligo(dT) priming using a template-switch primer 5′-AAGCAGTGGTATCAACGCAGAGTAC[T]20VN-3′ (47). Amplification of oligo(dT)-primed cDNAs was performed by PCR (Advantage II pol; BD Biosciences — Clontech) (40 cycles: 95°C 30 s, 68°C 3 min) using forward 5′-GGTTCCAAGTCCAATATGGCAA-3′ and reverse 5′-ACTAGGCATGTTCAGTGAAGGAGC-3′ primers for *LDH*, forward 5′-CAAGATGGCGGACCTGGA-3′ and reverse 5′-GGGTTGGTGCAGCAGGA-3′ primers for *GRK2*, forward 5′-CCGCCAAAGCTCGCCAAC-3′ and reverse 5′-ATCAGATGCCTCATCCTCGTTCAC-3′ primers for *GRK3*, forward 5′-GCTCCGTTGCTGACCGC-3′ and reverse 5′-CACTGTGGACTTGGAGGC-3′ primers for *GRK5*, and forward 5′-GCCACAGCCCATGGAGC-3′ and reverse 5′-AGCTGCTACCGCCAACTGCT-3′ primers for *GRK6*. For RNA synthesis and stability assays, cells were treated with 10 μg/ml ActD (Sigma-Aldrich) for 0–4 h before RNA isolation. mRNA half-lives were determined by fitting exponential decay curves to experimental data points. Primer pairs for quantitative RT-PCR were retrieved on the PrimerBank Web site (http://pga.mgh.harvard.edu/primerbank/) (48). PCR reactions were performed with SYBR Green (Applied Biosystems) detection using forward 5′-CTCGGGCCACTTCACTGAC-3′ and reverse 5′-CAGTCCGTACCTACCGATGTAT-3′ primers for *α–L-iduronidase* (*IDUA*), forward 5′-ACTTCAGCGTGCATCGCAT-3′ and reverse 5′-GCTTTTTGTCCAGGCACTTCAT-3′ primers for *GRK2*, forward 5′-AGCTGTAGAACACGTACAAAGTC-3′ and reverse 5′-ATGTCACCTCGAAGGCTTTCA-3′ primers for *GRK3*, and forward 5′-TAGCGAACACGGTGCTACTC-3′ and reverse 5′-GCTGATGTGAGGGAACTGGA-3′ primers for *GRK6*. We used the ABI 7300 Sequence Detection System (Applied Biosystems) with the following amplification scheme: 50°C 2 min, 95°C 10 min and 40 cycles: 95°C 15 s, 60°C 30 s, 68°C 40 s. The dissociation curve method was applied according to the manufacturer's protocol (60°C to 95°C) to ensure the presence of a single specific PCR product. Analysis was performed with the standard curve method, and results were expressed as *GRK*/*IDUA* ratios.

IB analysis. Equivalent amounts of proteins (30 μg/lane unless specified) were separated by SDS-PAGE on 4%–12% Tris-glycine polyacrylamide gels (Invitrogen), transferred to PVDF membrane and probed with the following monoclonal or polyclonal Abs: sheep anti-human LDH (Biodesign), rabbit anti-human β-arrestin1 (clone E246; Epitomics), rabbit anti-serum to β-arrestin2 (a gift from R.J. Lefkowitz, Howard Hughes Medical Institute, Durham, North Carolina, USA), rabbit anti-human GRK2 or -6, goat anti-human GRK3 (all from Santa Cruz Biotechnology Inc.), mouse anti-rat GRK2/3 (clone C5/1) or anti-bovine GRK5/6 (clone A16/17, both provided by M. Oppermann) Abs. Peroxidase-conjugated anti-mouse, anti-rabbit (both from Amersham Biosciences) and anti-goat (Vector Laboratories) Abs were used to detect bound primary Abs by enhanced chemiluminescence. IB quantitation was done using an LAS-1000 CCD camera with Image Gauge 3.4 software (Fuji Photo Film Co.).

Immunoprecipitation assay. Cells (5×10^6 to 10×10^6) transduced or not with $CXCR4^{WT}$ or $CXCR4^{1013}$ were serum-starved overnight and lysed in 0.2 ml ice-cold lysis buffer (LB; 30 mM HEPES, 100 mM KCl, 20 mM NaCl, 2 mM $MgCl_2$, 5% glycerol, 2% heptanetriol [Fluka], 0.5% laurylmaltoside, 5 mM GDP, 1 mM microcystin [Sigma-Aldrich], 1 mM orthovanadate and protease inhibitors [Roche Diagnostics]) for 30 min at 4°C. Precleared lysates were incubated overnight at 4°C with the 12G5 anti-CXCR4 mAb precoated on γ-bind sepharose beads (Amersham). After 3 washes in LB, immunoprecipitated receptors were eluted in SDS-PAGE sample buffer (25 mM Tris-HCl pH 6.8, 5% glycerol, 1.5% SDS, 0.1% bromophenol blue) for 45 min at 37°C and detected by IB analysis using the SZ1567 anti-CXCR4 rabbit polyclonal Ab (provided by M. Thelen).

Acknowledgments

This work was supported by Ensemble Contre le SIDA (SIDACTION), INSERM, the GIS-Network for Rare Diseases, the Ligue contre le Cancer, and the Agence Nationale de Recherches sur le SIDA (ANRS). K. Balabanian was supported by a Young Investigator Fellowship from INSERM, A. Levoye by a fellowship from the GIS-Network for Rare Diseases, and J. Harriague by a grant from the ANRS. We thank P. Bordigoni (Unité de Transplantation Médullaire, Centre Hospitalo-Universitaire de Nancy, Vandoeuvre-Les-Nancy, France) for providing us with blood samples from P4 and are grateful to C. Picard (Laboratoire CEDI, Pavillon Kirmisson, Hôpital Necker-Enfants Malades, Paris, France) for deriving fibroblasts and B cell lines from $WHIM^{WT}$ patients. We thank C. Bellanné-Chantelot for helpful discussions and S. Beaufils for technical assistance (Département de Génétique, Hôpital Pitié-Salpêtrière, Paris, France). We are grateful to T. Planchenault and L. Burleigh (INSERM U819, Laboratoire de Pathogénie Virale Moléculaire, Institut Pasteur, Paris, France) for technical help and critical reading of the manuscript, respectively.

Received for publication July 3, 2007, and accepted in revised form December 19, 2007.

Address correspondence to: Françoise Bachelerie, INSERM U819, Laboratoire de Pathogénie Virale Moléculaire, Institut Pasteur, 28 rue du Docteur Roux, Paris 75724, France. Phone: 33-0-1-40-61-34-67; Fax: 33-0-1-45-68-89-41; E-mail: fbachele@pasteur.fr.

Karl Balabanian's present address is: INSERM U764, Université Paris-Sud 11, Faculté de Médecine Paris Sud, Institut Fédératif de Recherche 13, Clamart, France.

1. Gorlin, R.J., et al. 2000. WHIM syndrome, an autosomal dominant disorder: clinical, hematological, and molecular studies. *Am. J. Med. Genet.* **91**:368–376.
2. Diaz, G.A. 2005. CXCR4 mutations in WHIM syndrome: a misguided immune system? *Immunol. Rev.* **203**:235–243.
3. Hernandez, P.A., et al. 2003. Mutations in the chemokine receptor gene CXCR4 are associated with WHIM syndrome, a combined immunodeficiency disease. *Nat. Genet.* **34**:70–74.
4. Premont, R.T., and Gainetdinov, R.R. 2007. Physiological roles of G protein-coupled receptor kinases and arrestins. *Annu. Rev. Physiol.* **69**:511–534.
5. Busillo, J.M., and Benovic, J.L. 2007. Regulation of CXCR4 signaling. *Biochim. Biophys. Acta.* **1768**:952–963.
6. Balabanian, K., et al. 2005. WHIM syndromes with different genetic anomalies are accounted for by impaired CXCR4 desensitization to CXCL12. *Blood.* **105**:2449–2457.
7. Moore, C.A., Milano, S.K., and Benovic, J.L. 2007. Regulation of receptor trafficking by GRKs and arrestins. *Annu. Rev. Physiol.* **69**:451–482.
8. Orsini, M.J., Parent, J.L., Mundell, S.J., Benovic, J.L., and Marchese, A. 1999. Trafficking of the HIV coreceptor CXCR4. Role of arrestins and identification of residues in the c-terminal tail that mediate receptor internalization. *J. Biol. Chem.* **274**:31076–31086.
9. Cheng, Z.J., et al. 2000. beta-arrestin differentially regulates the chemokine receptor CXCR4-mediated signaling and receptor internalization, and this implicates multiple interaction sites between beta-arrestin and CXCR4. *J. Biol. Chem.* **275**:2479–2485.
10. Fong, A.M., et al. 2002. Defective lymphocyte chemotaxis in beta-arrestin2- and GRK6-deficient mice. *Proc. Natl. Acad. Sci. U. S. A.* **99**:7478–7483.
11. Rey, M., et al. 2007. Myosin IIA is involved in the endocytosis of CXCR4 induced by SDF-1alpha. *J. Cell Sci.* **120**:1126–1133.
12. Haribabu, B., and Snyderman, R. 1993. Identification of additional members of human G-protein-coupled receptor kinase multigene family. *Proc. Natl. Acad. Sci. U. S. A.* **90**:9398–9402.
13. De Blasi, A., Parruti, G., and Sallese, M. 1995. Regulation of G protein-coupled receptor kinase subtypes in activated T lymphocytes. Selective increase of beta-adrenergic receptor kinase 1 and 2. *J. Clin. Invest.* **95**:203–210.
14. Metaye, T., Gibelin, H., Perdrisot, R., and Kraimps, J.L. 2005. Pathophysiological roles of G-protein-coupled receptor kinases. *Cell Signal.* **17**:917–928.
15. Vroon, A., et al. 2004. GRK6 deficiency is associated with enhanced CXCR4-mediated neutrophil chemotaxis in vitro and impaired responsiveness to G-CSF in vivo. *J. Leukoc. Biol.* **75**:698–704.
16. Balabanian, K., et al. 2005. The chemokine SDF-1/CXCL12 binds to and signals through the orphan receptor RDC1 in T lymphocytes. *J. Biol. Chem.* **280**:35760–35766.
17. Bhandari, D., Trejo, J., Benovic, J.L., and Marchese, A. 2007. Arrestin-2 interacts with the E3 ubiquitin ligase AIP4 and mediates endosomal sorting of the chemokine receptor CXCR4. *J. Biol. Chem.* **282**:36971–36979.
18. Haribabu, B., et al. 1997. Regulation of human chemokine receptors CXCR4. Role of phosphorylation in desensitization and internalization. *J. Biol. Chem.* **272**:28726–28731.
19. Amara, A., et al. 1997. HIV coreceptor downregulation as antiviral principle: SDF-1alpha-dependent internalization of the chemokine receptor CXCR4 contributes to inhibition of HIV replication. *J. Exp. Med.* **186**:139–146.
20. Signoret, N., et al. 1997. Phorbol esters and SDF-1 induce rapid endocytosis and down modulation of the chemokine receptor CXCR4. *J. Cell Biol.* **139**:651–664.
21. Roland, J., et al. 2003. Role of the intracellular domains of CXCR4 in SDF-1-mediated signaling. *Blood.* **101**:399–406.
22. Kawai, T., et al. 2005. Enhanced function with decreased internalization of carboxy-terminus truncated CXCR4 responsible for WHIM syndrome. *Exp. Hematol.* **33**:460–468.
23. Signoret, N., et al. 1998. Differential regulation of CXCR4 and CCR5 endocytosis. *J. Cell Sci.* **111**:2819–2830.
24. Woerner, B.M., Warrington, N.M., Kung, A.L., Perry, A., and Rubin, J.B. 2005. Widespread CXCR4 activation in astrocytomas revealed by phospho-CXCR4-specific antibodies. *Cancer Res.* **65**:11392–11399.
25. Ferguson, S.S., et al. 1996. Role of beta-arrestin in mediating agonist-promoted G protein-coupled receptor internalization. *Science.* **271**:363–366.
26. Kim, J., et al. 2005. Functional antagonism of different G protein-coupled receptor kinases for beta-arrestin-mediated angiotensin II receptor signaling. *Proc. Natl. Acad. Sci. U. S. A.* **102**:1442–1447.
27. Ren, X.R., et al. 2005. Different G protein-coupled receptor kinases govern G protein and beta-arrestin-mediated signaling of V2 vasopressin receptor. *Proc. Natl. Acad. Sci. U. S. A.* **102**:1448–1453.
28. Ribas, C., et al. 2007. The G protein-coupled receptor kinase (GRK) interactome: Role of GRKs in GPCR regulation and signaling. *Biochim. Biophys. Acta.* **1768**:913–922.
29. Peppel, K., et al. 1997. G protein-coupled receptor kinase 3 (GRK3) gene disruption leads to loss of odorant receptor desensitization. *J. Biol. Chem.* **272**:25425–25428.
30. Walker, J.K., Peppel, K., Lefkowitz, R.J., Caron, M.G., and Fisher, J.T. 1999. Altered airway and cardiac responses in mice lacking G protein-coupled receptor kinase 3. *Am. J. Physiol.* **276**:R1214–R1221.
31. Xu, M., et al. 2004. Neuropathic pain activates the endogenous kappa opioid system in mouse spinal cord and induces opioid receptor tolerance. *J. Neurosci.* **24**:4576–4584.
32. Wright, N., et al. 2002. The chemokine stromal cell-derived factor-1 alpha modulates alpha 4 beta 7 integrin-mediated lymphocyte adhesion to mucosal addressin cell adhesion molecule-1 and fibronectin. *J. Immunol.* **168**:5268–5277.
33. Tan, W., Martin, D., and Gutkind, J.S. 2006. The Galpha13-Rho signaling axis is required for SDF-1-induced migration through CXCR4. *J. Biol. Chem.* **281**:39542–39549.
34. Rochdi, M.D., and Parent, J.L. 2003. Galphaq-coupled receptor internalization specifically induced by Galphaq signaling. Regulation by EBP50. *J. Biol. Chem.* **278**:17827–17837.
35. Shi, G., et al. 2007. Identification of an alternative G{alpha}q-dependent chemokine receptor signal transduction pathway in dendritic cells and granulocytes. *J. Exp. Med.* **204**:2705–2718.
36. Sun, Y., Cheng, Z., Ma, L., and Pei, G. 2002. Beta-arrestin2 is critically involved in CXCR4-mediated chemotaxis, and this is mediated by its enhancement of p38 MAPK activation. *J. Biol. Chem.* **277**:49212–49219.
37. Violin, J.D., Ren, X.R., and Lefkowitz, R.J. 2006. G-protein-coupled receptor kinase specificity for beta-arrestin recruitment to the beta2-adrenergic receptor revealed by fluorescence resonance energy transfer. *J. Biol. Chem.* **281**:20577–20588.
38. Potter, R.M., Maestas, D.C., Cimino, D.F., and Prossnitz, E.R. 2006. Regulation of N-formyl peptide receptor signaling and trafficking by individual carboxyl-terminal serine and threonine residues. *J. Immunol.* **176**:5418–5425.
39. Dautzenberg, F.M., Braun, S., and Hauger, R.L. 2001. GRK3 mediates desensitization of CRF1 receptors: a potential mechanism regulating stress adaptation. *Am. J. Physiol. Regul. Integr. Comp. Physiol.* **280**:R935–R946.
40. Wang, J., et al. 2001. Role of tyrosine phosphorylation in ligand-independent sequestration of CXCR4 in human primary monocytes-macrophages. *J. Biol. Chem.* **276**:49236–49243.
41. Dautzenberg, F.M., Wille, S., Braun, S., and Hauger, R.L. 2002. GRK3 regulation during CRF- and urocortin-induced CRF1 receptor desensitization. *Biochem. Biophys. Res. Commun.* **298**:303–308.
42. McLaughlin, J.P., et al. 2004. Prolonged kappa opioid receptor phosphorylation mediated by G-protein receptor kinase underlies sustained analgesic tolerance. *J. Biol. Chem.* **279**:1810–1818.
43. Salim, S., Standifer, K.M., and Eikenburg, D.C. 2007. Extracellular signal-regulated kinase 1/2-mediated transcriptional regulation of G-protein-coupled receptor kinase 3 expression in neuronal cells. *J. Pharmacol. Exp. Ther.* **321**:51–59.
44. Niculescu, A.B., 3rd, et al. 2000. Identifying a series of candidate genes for mania and psychosis: a convergent functional genomics approach. *Physiol. Genomics.* **4**:83–91.
45. Barrett, T.B., et al. 2003. Evidence that a single nucleotide polymorphism in the promoter of the G protein receptor kinase 3 gene is associated with bipolar disorder. *Mol. Psychiatry.* **8**:546–557.
46. Balabanian, K., et al. 2004. CXCR4-tropic HIV-1 envelope glycoprotein functions as a viral chemokine in unstimulated primary CD4+ T lymphocytes. *J. Immunol.* **173**:7150–7160.
47. Matz, M., et al. 1999. Amplification of cDNA ends based on template-switching effect and step-out PCR. *Nucleic Acids Res.* **27**:1558–1560.
48. Wang, X., and Seed, B. 2003. A PCR primer bank for quantitative gene expression analysis. *Nucleic Acids Res.* **31**:e154.